Generalized Wigner lattices in one dimension and some applications to tetracyanoquinodimethane (TCNQ) salts

J. Hubbard

IBM Research Laboratory, San Jose, California 95193
(Received 7 September 1977)

Estimates show that both the on-site and the near-neighbor electrostatic interactions in tetracyanoquinodimethane chains may be much greater than the bandwidth. A method of determining the exact ground state when the interactions are dominant is described; the electrons are found to have a periodic arrangement which may be regarded as a generalization of the classical Wigner lattice. It is shown how the optical spectra may be interpreted in terms of such a configuration; also that such arrangements may give rise to lattice distortions manifested as satellites in the x-ray diffraction pattern.

I. INTRODUCTION

In recent years there has been much interest in quasi-one-dimensional conductors. In many of these compounds the conduction bands are quite narrow [e.g., 0.5–1.5 eV in tetracyanoquinodimethane TCNQ) salts[1,2]], which has led to speculation that the Coulomb interactions may be playing an important role. In particular, Torrance *et al.*[3,4] and Soos[5] have argued that the on-site interaction in TCNQ salts may be large enough to make a Hubbard model[6] appropriate. However, the physical reasoning[6] that supports the application of the Hubbard model to, say, the d electrons of transition metals, may not be valid for the conduction electrons of TCNQ chains. For the d electrons it was argued that the bandwidth was small compared to the on-site interaction but large relative to the interatomic d-electron interaction. In the case of a TCNQ chain, simple electrostatic considerations (discussed in Sec. II) suggest, on the contrary, that not only the on-site interaction, but also several near-neighbor interactions are large compared to the bandwidth, leading to an essentially new physical situation. In fact, nearest-neighbor and more-distant interactions have been considered by various authors (e.g., Ovchinnikov[7] and Kondo and Yamaji[8]); it is the main purpose of this paper to investigate these matters further.

Of course, the introduction of many interactions leads to a rather difficult many-body problem. In order to gain some insight into the nature of the solutions, we have adopted the strategy which was originally used[6] in connection with the Hubbard model, namely, to investigate first the zero-bandwidth limit and then attempt to graft on the effects of band motion later. The solution of the Hubbard model in the zero-bandwidth limit is rather trivial, but this is not so in the present case. In this limit, apart from the interaction strengths, there is one other parameter, the electron transfer ρ.

The problem (see Sec. II) reduces to: How is one to distribute ρN electrons over the N sites of a TCNQ chain so as to minimize the interaction energy? An exact solution has been found for this problem for a rather wide class of interactions; this solution is described in Sec. III, and some related proofs are given in the Appendix. The electron arrangement in the ground state is found to be periodic, the period and the precise arrangement of the electrons within a period depending on the parameter ρ. These arrangements may be regarded as one-dimensional generalizations of the classical Wigner lattice[9] which is the configuration adopted by a very-low-density electron gas in three dimensions.

Because of the zero-bandwidth assumption, one cannot regard this solution as a very realistic model of a real TCNQ chain. Nevertheless, if the interaction effects are of dominant importance, some features of the model may well survive the introduction of a finite bandwidth (see Sec. VI). It is, in fact, found that, going no farther than this model, one can obtain an interpretation of the optical spectra of many TCNQ salts; indeed, similar models[10] have already been proposed in this connection. In Sec. IV an example, that of tetrathiofulvalene (TTF)-TCNQ, is discussed.

In general, the arrangement of the electrons within a period of the generalized Wigner lattice is nonuniform. This nonuniformity will give rise to electric fields which can distort the ordinary lattice. These distortions may manifest themselves as satellites in the x-ray diffraction pattern. In Sec. V the strengths of these satellites have been estimated. Whilst many satellites are potentially possible, it is found that all but a few are of negligible intensity. The positions of the strong satellites have been located as a function of ρ. For $\rho > \frac{1}{2}$, a strong satellite is generally found at the $4k_F$ position, and in some cases harmonics of this satellite are also found.

In Sec. VI the effects of the reintroduction of a finite bandwidth are considered. Some indication is obtained of the parameter regime within which the interactions may be considered to be dominant. The way in which the results relating to the optical spectra and the x-ray satellites may be modified is discussed, and some new phenomena, such as conduction by a "dimer gas," are described. In general, however, it is concluded that better solutions are required.

II. FORMULATION OF THE MODEL

Consider a TCNQ chain in, say, TTF-TCNQ. One is interested in the band containing the transferred electrons which arises from a single orbital of the TCNQ molecule. Since the overlap of these orbitals is very small,[1,2] a tight-binding model is appropriate. A suitable Hamiltonian for such a band is

$$H = t \sum_{i\sigma} (c^\dagger_{i+1,\sigma} c_{i\sigma} + c^\dagger_{i\sigma} c_{i+1,\sigma})$$
$$+ \tfrac{1}{2} \sum_{i \neq j} V_{i-j} n_i n_j + \tfrac{1}{2} \sum_{i,\sigma} U n_{i\sigma} n_{i,-\sigma}, \qquad (1)$$

where $c_{i\sigma}$ is the destruction operator for an electron of spin σ in the molecular orbital at site i, $n_{i\sigma} = c^\dagger_{i\sigma} c_{i\sigma}$ is the occupation number of this state, $n_i = \sum_\sigma n_{i\sigma}$ is the operator giving the total number of electrons at site i, t is the transfer integral between nearest-neighbor sites, U is the interaction of two electrons on the same site, and $V_n = V_{-n}$ is the interaction of electrons on nth-nearest-neighbor sites. The sums over i, j in (1) are over all the sites of the one-dimensional chain; the first term of (1) would by itself give rise to a tight-binding band with width $4t$; the other terms represent the interaction.

The importance of the interactions will be measured by the magnitudes of the parameters $U, V_1, V_2, \ldots$, relative to the bandwidth $4t$. We therefore try to estimate these parameters. Since this material is a conductor and contains highly polarizable molecules, one may expect screening effects to be of great importance. Nevertheless, we first estimate these parameters neglecting screening. The unscreened U is given by the dis-

proportionation energy for the reaction $2TCNQ^- \rightarrow TCNQ + TCNQ^{2-}$, for which Johansen's calculations[11] give the value $U \simeq 4.5$ eV. The unscreened V_n may be calculated as the electrostatic interaction of the charge distributions on nth-neighbor TCNQ ions of the TCNQ chain; using the charge distribution given by Johansen,[11] one obtains the values given in Table I, column 2. One may note from these values that not only U but the V_n for the several near neighbors are greater than the bandwidth $4t \simeq 0.5$ eV, so very complete screening in necessary to render them unimportant. This situation contrasts with that encountered in some other narrow energy-band materials, such as transition and rare-earth metals, where it can be plausibly argued that U is greater than the bandwidth but that neighbor interactions are much smaller.[6] Here it appears that the neighbor interaction may also be important.

How are these conclusions modified when the screening is taken into account? It is first necessary to be clear what is meant by screening in the context of the Hamiltonian (1). The motion of the conduction electrons on the chain under consideration would screen any charge. However these effects will emerge in the solution of the problem posed by (1) and are not to be taken into account separately in setting up this Hamiltonian. Thus in determining the parameters in (1) one must take into account only the screening due to electrons other than the conduction electrons of that particular chain, namely the screening by conduction and polarization of neighboring chains and by the polarization of the nonconduction ("core") electrons of the chain itself.

Some rough estimates have been made of these screening effects. Consider first the screening by conduction on neighboring chains. This may be approximately represented by recalculating the Coulomb interactions for a chain enclosed in a cylindrical hole in a perfectly conducting medium. If the radius of the hole is R, straightforward electrostatic calculations show that U will be reduced by approximately $\pi e^2/4R$ and V_n by a factor $e^{-nd/R}$, where d is the nearest-neighbor distance. Taking $R = 8.45 A$, an appropriate value for TTF-TCNQ, gives the results shown in Table I, column 3.

TABLE I. Estimates (in eV) of screened interactions on a TCNQ chain.

Interaction	Unscreened	Screened by conduction	Screened by polarization	Totally screened
U	4.5	3.2		2.4
V_1	2.54	1.62	1.15	0.9
V_2	1.56	0.63	0.71	0.35
V_3	1.09	0.22	0.5	0.12

The effect of polarization screening on the V_n can be represented approximately by reducing them by a factor $1/\epsilon$, where (out to about the fourth nearest neighbors) ϵ should be the "background" dielectric constant $\simeq 2.2$; the effects ("exaltations" of polarizability, see, e.g., Ref. 12) which make the measured dielectric constant of, say, solid TCNQ much greater than 2 are associated with extended molecular orbitals and are found to be ineffective in screening near-neighbor interactions because the electric fields involved vary rapidly over the extent of the orbital. If one takes $\epsilon = 2.2$, the values shown in Table I, column 4, are obtained.

Finally, one should consider the two screening mechanisms in combination. They are not additive; on the contrary, each reduces the effectiveness of the other. Estimates have been made of the combined effect and are shown in column 5 of Table I. How these estimates were obtained will not be discussed here since it is hoped in the near future to give an account of more precise calculations of this kind at present in progress.

The figures in column 5 of Table I show that the on-site and the neighbor interactions out to the third nearest neighbors are greater than $2t \simeq 0.25$ eV (this is the appropriate comparison as is shown in Sec. VI). The remainder of this paper is devoted to exploring some of the consequences of such strong interactions.

The solution of the Hamiltonian (1) with large U and V presents a formidable problem. Since the biggest energies involved are these interactions, one approach would be to investigate the solutions at $t = 0$, i.e., in the zero-bandwidth limit, and to try and treat the band-motion effects by perturbation theory; this is the method employed here. If one puts $t = 0$ in (1), one is left with the Hamiltonian

$$H = \tfrac{1}{2}\sum_{i,\sigma} U n_{i\sigma} n_{i,-\sigma} + \tfrac{1}{2}\sum_{i \neq j} V_{i-j} n_i n_j , \qquad (2)$$

the solution of which is not enirely trivial; it is the problem which will first be studied.

The problem presented by (2) is classical, i.e., not quantum mechanical. The determination of the ground state amounts to enquiring how one is to distribute ρN electrons over the $2N$ orbitals of a chain of length N so as to minimize the interaction energy (2), where ρ is the electron density

$$\rho N = \sum_{i,\sigma} c_{i\sigma}^\dagger c_{i\sigma} ; \qquad (3)$$

ρ is, for example, the number of electrons transferred per molecule in TTF-TCNQ.

One may make certain simplifications at once. It is expected, in practice, that $\rho \lesssim 1$ (and even if

$\rho \lesssim 1$ one could transform the problem to a similar one with $\rho < 1$ by interchanging electrons and holes). If $\rho \lesssim 1$ it is possible for the electrons to arrange themselves so that there is no double occupancy, i.e., no site has both an up- and a down-spin electron. If U is much larger than the V_n, one would expect that in the ground state of (2) there would be no double occupancy; in fact, one may show by a generalization of the arguments of the Appendix that this will be so provided

$$U + V_2 > 2V_1 \qquad (4)$$

is satisfied. Condition (4) is satisfied by all the parameter sets given in Table I, so it will be assumed that there is no double occupancy. In this case one may dispense with the spin labeling altogether and reduce the problem to that of minimizing

$$H = \tfrac{1}{2}\sum_{i \neq j} V_{i-j} n_i n_j , \qquad (5)$$

subject to the condition

$$\rho N = \sum_i n_i , \qquad (6)$$

where the n_i may now take the values 0 or 1 (each site is empty or singly occupied). This is the problem to be studied in Sec. III. It has been previously investigated by Kondo and Yamaji[8] in connection with the x-ray scattering discussed in Sec. V; they employed a Monte Carlo method to determine the probability of various configurations $\{n_i\}$ at finite temperatures for several values of ρ.

It may be remarked in connection with some later developments (see Sec. VI) that (5) and (6) are equivalent to a certain one-dimensional Ising-model problem if one re-interprets the $n_i = 0$ and $n_i = 1$ as down and up spins; the equivalent problem is that of finding the lowest-energy state of an Ising lattice with a prescribed magnetization [given by (6)] and many-neighbor interactions.

III. GENERALIZED WIGNER LATTICES

It is sufficient to obtain the ground state of (5) and (6) for $\rho \leq \tfrac{1}{2}$; for one may obtain the solution for any density ρ from that at density $1-\rho$ by merely interchanging electrons and holes.

The ground state has not been obtained for arbitrary V_n, but for a particular class of potentials, namely, those satisfying the two conditions

$$V_n \to 0 \quad \text{as } n \to \infty , \qquad (7)$$

$$V_{n+1} + V_{n-1} \geq 2V_n \quad \text{for all } n > 1 . \qquad (8)$$

The first condition is rather easily accepted. The second requires that the potential be convex down-

TABLE II. Generalized-Wigner-lattice configurations.

	Density	Period		Configuration
(a)	$\frac{1}{3}$	3	3	100100100...
(b)	$\frac{2}{5}$	5	32	100101001010010...
(c)	$\frac{3}{7}$	7	$2^2 3$	10101001010100...
(d)	$\frac{3}{8}$	8	$3^2 2$	1001001010010010...
(e)	$\frac{10}{23}$	23	$(2^2 3)^2 2^3 3$	10101001010100101010100...
(f)	$\frac{3}{5}$	5	12^2	1101011010...
(g)	$\frac{3}{4}$	4	$1^2 2$	111011101110...
(h)	$\frac{4}{7}$	7	12^3	1101010101101010...
(i)	$\frac{1}{2}$	2	2	1010101010...
(j)	$\frac{1}{2}$	4	13	110011001100...

wards; it is satisfied, for example, by the ordinary Coulomb potential, and by all the potentials given in Table I.

The ground-state configurations for $\rho \leqslant \frac{1}{2}$ may be described as follows (the proofs of the various statements are outlined in the Appendix). If $\rho = \frac{1}{2}, \frac{1}{3}, \ldots, 1/n, \ldots$ (n is an integer), it is easy to see that for a Coulomb potential the lowest-energy configuration is that in which all the electrons are equally spaced a distance n neighbors apart; this is the one-dimensional analogue of the classical Wigner lattice[9] which is the ground state of a very-low-density electron gas in three dimensions.

Suppose now that ρ does not take one of the special values $1/n$. The next simplest case is that in which ρ has the form $\frac{2}{5}, \frac{2}{7}, \ldots, 2/2n+1, \ldots$ (n is an integer), in which case the electrons arrange themselves alternately at intervals of n and $n+1$ [see, e.g., Table II, line (b)]. In fact, for any density ρ between $1/n$ and $1/(n+1)$ the intervals between electrons are always equal to either n or $n+1$. For densities of the special form

$$\rho = (m+1)/(mn+n+1) = [n+1/(m+1)]^{-1}, \quad (9)$$

where n,m are integers, the arrangement consists of periodically repeating configuration with period $nm+n+1$, the $m+1$ electrons in each period arranging themselves with m intervals n and one interval $n+1$ [see, e.g., Table II, line (c)]; we introduce the notation $n^m(n+1)$ for this arrangement and ρ_{nm} for the corresponding density given by (9).

For densities of the form

$$\rho = (m+1)/(mn+n-1) = [n-1/(m+1)]^{-1}, \quad (10)$$

where n,m are integers, the period is $mn+n-1$ and the $m+1$ electrons in each period are ar-

ranged with m intervals of n and one interval of $n-1$, i.e., according to $n^m(n-1)$ [see, e.g., Table II, line (d)].

For ρ not given by (9) or (10) the arrangements are more complicated. For example, if the density ρ is between ρ_{nm} and $\rho_{n,m+1}$ the configuration is entirely made up of sequences of the form $n^m(n+1)$ and $n^{m+1}(n+1)$ and, for example, for densities ρ of the particular form

$$1/\rho = n + (p+1)/[p(m+1)+m+2], \quad (11)$$

where n,m,p are integers the periodically repeating unit consists of the sequence $n^m(n+1)$ repeated p times followed by the sequence $n^{m+1}(n+1)$, i.e., is $[n^m(n+1)]^p n^{m+1}(n+1)$ [see, e.g., Table II, line (e)].

In fact, guided by the considerations of the Appendix, one may find the configurations corresponding to any rational value of ρ. The configuration corresponding to the value $\rho = p/q$ (p,q are integers with no common factor) is periodic with period q and p electrons in each period. The arrangement of the electrons in each period may be determined by the following algorithm:

(i) Define the integers $k, n, n_1, n_2, \ldots, n_k$ by the following equations:

$$1/\rho = n + r_0,$$

$$|1/r_0| = n_1 + r_1,$$

$$|1/r_1| = n_2 + r_2,$$

$$\vdots$$

$$|1/r_{k-2}| = n_{k-1} + r_{k-1},$$

$$|1/r_{k-1}| = n_k,$$

where for all s, $-\frac{1}{2} < r_s \leqslant \frac{1}{2}$ (the sequence must terminate for rational ρ).

(ii) Define the sequences $X_1, X_2, \ldots, X_k$ and Y_1, $Y_2, \ldots, Y_k$ by

$$X_1 = n,$$

$$Y_1 = n + \alpha_0,$$

$$X_{i+1} = [X_i]^{n_i - 1} Y_i,$$

$$Y_{i+1} = [X_i]^{n_i + \alpha_i - 1} Y_i,$$

where $\alpha_i = r_i / |r_i| = \pm 1$.

(iii) Then the required arrangement in each period is given by X_k.

For example, if $\rho = \frac{11}{47}$, the period is 47 with 11 electrons in each period, $n = 4, n_1 = 4, n_2 = 3, \alpha_0 = 1$, $\alpha_1 = -1, X_1 = 4, Y_1 = 5, X_2 = 4^3 5, Y_2 = 4^2 5$ and the arrangement in each period is $(4^3 5)^2 4^2 5 = 44454445445$, where the $4s$ and $5s$ indicate the spacings between successive electrons in each period.

Once the configurations have been obtained for $\rho < \frac{1}{2}$ by the above algorithm, those for $\rho > \frac{1}{2}$ can be obtained by interchanging electrons and holes; some are shown in Table II. The periodic configurations obtained in this way will be referred to as generalized Wigner lattices.

The possibility that the interactions might cause a tendency for the electrons to arrange themselves in such patterns has been previously suggested in various contexts. In the theory of charge-density waves the discommensuration idea of McMillan[13] has some similarity, and a somewhat similar picture is mentioned by Lee, Rice, and Klemm.[14] As discussed in Sec. IV, this kind of model has been used in connection with the interpretation of optical spectra,[10] and Silverman and Torrance have considered the role of Wigner lattice formation in connection with cohesive energy calculations.[15]

A comment is in order on the role of the convexity condition (8). It is shown in the Appendix that (8) is a sufficient condition to guarantee the ground-state configurations described above. If it is not satisfied, the ground state may be of a different kind. Consider, for example, the case $\rho = \frac{1}{2}$ with $0 = V_3 = V_4 = \cdots$. If $V_1 > 2V_2$, then (8) is satisfied and the ground state is the Wigner lattice of period 2 [Table II, line (i)]; but if $V_1 < 2V_2$, and (8) is not satisfied, one may easily convince oneself that the ground state is the period 4 configuration given in Table II, line (j). This comment may not be entirely academic. Inspection of column 5 of Table I shows that whilst (8) is satisfied, fairly modest variations could cause (8) to fail. Thus it would seem quite possible that in some materials with $\rho = \frac{1}{2}$ the arrangement of Table II, line (j) might be preferred, and, indeed, some tetramerized materials with $\rho = \frac{1}{2}$ are known.

We finally remark that what was obtained above is the ground-state configuration. At finite tem-

perature T one cannot have such configurations with long-range order in one dimension. For finite and small enough T the typical configuration will consist of regions of the appropriate generalized Wigner lattice separated by "faults" where phase slippage occurs, destroying the long-range order, but leaving generalized-Wigner-lattice configurations locally.

IV. OPTICAL SPECTRA

It has been found that one may interpret the optical spectra of many of the charge-transfer salts of TCNQ in terms of the configurations of Sec. III, and, indeed, models closely resembling those of Sec. III have already been proposed in this connection.[10] One may illustrate the possibilities by considering the spectrum of TTF-TCNQ. Suppose, for simplicity, that in this case a value $\rho = 0.6$ is appropriate, so the ground state will, according to Sec. III, be that given in Table II, line (f), redrawn in Fig. 1(a). It may be noted that this structure can be considered as made up of neutral TCNQ molecules, isolated TCNQ$^-$ ions (i.e., TCNQ$^-$ ions with neutrals on each side) which will be called "monomers," and isolated pairs of TCNQ$^-$ ions to be called "dimers."

Two types of optical transition are of importance: intramolecular transitions in which an electron is excited to a higher level on the same molecule, which may be neutral, monomer, or dimer [A, B, C in Fig. 1(a)]; and charge-transfer transitions in which an electron is excited to a neighboring site, the three types of which are indicated by D, E, and F in Fig. 1(a). Information concerning the intramolecular spectra can be obtained from solution studies[16,17] on neutral TCNQ and TCNQ$^-$ ions in monomer and dimer configurations; such spectra are shown in Figs. 2(a) and 2(b). (Actually the dimer spectrum also contains a peak at $\simeq 1.3$ eV which should probably be assigned to a charge transfer transition of type F on the dimer pair.) One has no such direct information concerning the charge-transfer transitions (except that just mentioned) and must fall back on Hamiltonian (5) to estimate the energies of these transitions. Consider, for example, the transition D; this will lead
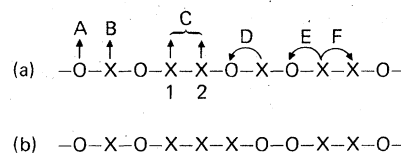
FIG. 1. Optical transitions in the case $\rho = 0.6$. (The crosses represent occupied sites, the circles empty sites.)
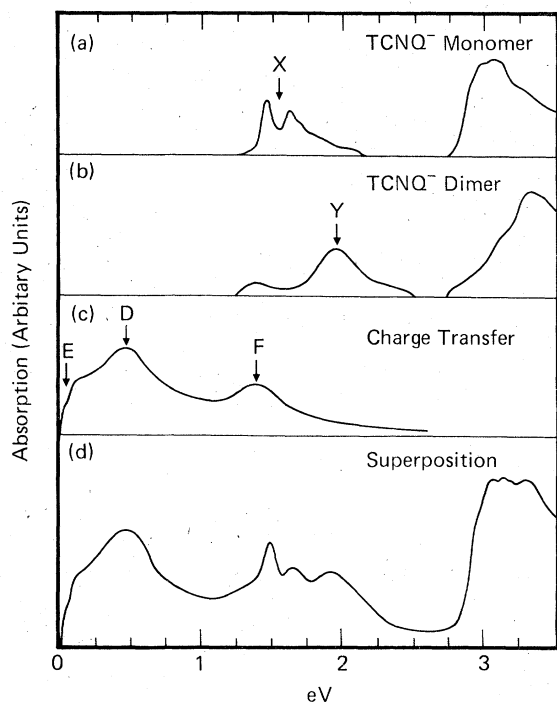
FIG. 2. Contributions to the optical spectrum of a TCNQ chain (see Sec. VI).

to the new configuration shown in Fig. 1(b), and, using Hamiltonian (5), one finds the difference in energy of the configurations of Figs. 1(a) and 1(b) to be $V_1 - V_2 - V_3 + 2V_4 + \cdots$, so the transition D should have about this energy. In this way one finds the transitions D, E, F to have energies $V_1 - V_2 - V_3 + \cdots$, $V_4 + \cdots$, and $U - V_1$, respectively; using the values of Table I, column 5, these energies are about 0.4, 0, and 1.5 eV, respectively. The corresponding spectrum has been sketched in Fig. 2(c), adding a broadening of about 0.5 eV to simulate the effects of band motion and vibrational broadening.

If one now superposes the spectra of the neutrals, monomers, dimers, and the charge-transfer spectrum in suitable proportions, one obtains the spectrum shown in Fig. 2(d), which is not unlike the observed spectrum of TTF-TCNQ.[3] Furthermore, the observed polarizations[18] are consistent with the model (charge-transfer transitions will be predominantly polarized along the stack direction, the intramolecular transitions perpendicular). Particularly noteworthy is the appearance of the characteristically split peak X associated with the monomer spectrum; according to the theory of Sec. III, this should be present in varying amounts for all $\rho < \frac{2}{3}$, but not, for example, at $\rho = 1$ as in the alkali salts of TCNQ (in which case there should be a single peak associated with the transition F at about

this energy; the peak X of the monomer spectrum falls fortuitously at about the same energy as transition F).

Of course, Fig. 2(d) would represent only the contribution to the optical spectrum from the TCNQ chain; one should add to it the corresponding contribution of the TTF chain. Using solution data[19] for neutral TTF and TTF⁻ (monomer and dimer), one would expect the TTF chain spectrum to look rather similar to Fig. 2(d) except that the peaks X, Y lie about 0.5 eV higher in TTF, thus tending to fill in the valley at around 2.5 eV in Fig. 2(d).

It has proved possible by similar discussion to give an interpretation of the spectra of many charge-transfer salts. However, the model is not without its difficulties. For example, in some salts (e. g., hexamethylene tetraselenafulvalene (HMTSF-TCNQ[20] and N-methylphenazinium (NMP)-TCNQ[3]) in which it is believed that $\rho > \frac{2}{3}$ the spectra show the double peak at an energy of $\simeq 1.3$ eV which was interpreted above as the monomer transition X; however, for the $\rho > \frac{2}{3}$ the generalized Wigner lattice has no monomer component.

It is not expected that the above interpretation will be much modified at ordinary temperatures by the appearance of the "faults" mentioned at the end of Sec. III. However, the introduction into the model of large enough bandwidth could cause significant changes; this point is discussed in Sec. VI.

V. LATTICE DISTORTIONS

If the electrons at, say $\rho = \frac{3}{5}$, did actually adopt the configuration of Fig. 1(a) (at least locally), then the lack of symmetry would lead to electric fields tending to displace the ions; for example, the repulsion of the charges on sites 1, 2 [Fig. 1(a)] would tend to push these ions apart. Thus the generalized-Wigner-lattice arrangements of the electrons would sometimes lead to lattice distortions which might manifest themselves as satellites in the x-ray diffraction pattern. Indeed, Kondo and Yamaji[8] have already studied this effect at finite temperatures for a few densities using a Monte Carlo technique to obtain the configuration. We propose here to use the generalized-Wigner-lattice results to investigate this effect. In fact, it will be shown that the distortions may lead to x-ray satellites at some of the positions (in particular $4k_F$ at which they have been observed experimentally.[28,29,30]

One should distinguish (see Ref. 8) between the distortions to be discussed here and those arising from a Peierls instability; the latter is brought about by a combination of the band motion and the Fermi statistics of the electrons. However, the

mechanism discussed here exists (indeed exists more strongly) when there is no band motion and the problem is essentially classical.

To investigate the distortion of the lattice, first note that if the ith site of a generalized Wigner lattice suffers a displacement u_i, then the energy changes, according to (5), by an amount

$$\Delta E = \sum_{i \neq j} n_i n_j V'_{i-j} u_i + O(u_i^2) ,$$ (12)

where

$$V'_{i-j} = \frac{dV(x)}{dx} \bigg|_{x = R_i - R_j} ,$$

$V(x)$ is the interaction potential, and R_i is the position of the ith site; the $\{n_i\}$ in (12) are the site occupation numbers corresponding to the generalized-Wigner-lattice configuration. Equation (12) shows that the force acting at the ith site is

$$F_i = n_i \sum_{j \neq i} V'_{i-j} n_j .$$ (13)

These forces will cause the lattice to distort by an amount determined by the resistance to them due to the ordinary intermolecular interactions; the simplest approach is to regard the forces (13) as giving rise to a (static) displacement δx_k of the phonon coordinate x_k (for simplicity the phonons are treated as one-dimensional; the generalization to three dimensions is straightforward). One may easily show that

$$M \omega_k^2 \delta x_k = \sum_j F_j e^{-ikR_j} ,$$ (14)

where ω_k is the phonon frequency and M the mass of a molecule. The corresponding displacement of the ith site due to the distortion is then given by

$$u_i = \sum_k \delta x_k e^{ikR_i} .$$ (15)

The strength of the X-ray scattering with wave vector Q is determined by $|F(Q)|^2$, where

$$F(Q) = g(Q) \sum_j e^{iQ(R_j + u_j)}$$

$$= g(Q) \sum_j e^{iQR_j} \left(1 + iQ \sum_k \delta x_k e^{ikR_j} + \cdots \right) ,$$ (16)

where $g(Q)$ is the molecular form factor, e^{iQu_j} has been expanded, and u_j substituted from (15). One sees at once from (16) that the distortion will give rise to satellites of the main spots displaced from them through distances k, where k is any wave vector for which δx_k is nonvanishing. If the generalized Wigner lattice has period p, then the forces F_i will be periodic with the same period, and, according to (14), δx_k will be nonvanishing provided k has the form

$$k = (m/p)b^* , \quad m = 1, 2, \ldots, p - 1 ,$$ (17)

where b^* is the basis vector of the reciprocal lattice. Thus, if p is large, one could potentially obtain a great many satellites; however, it is found that most satellites are of very low intensity and only a few are at all prominent (see below).

From (14)–(16) one finds that the intensity of a satellite with displacement k is proportional to

$$\left(\frac{Qg(Q)}{Mp\omega_k^2} \right)^2 \left| \sum_j^{(c)} F_j e^{-ikR_j} \right|^2 \equiv \left(\frac{Qg(Q)}{M\omega_k^2} \right)^2 |f(k)|^2 ,$$ (18)

where the sum $\sum_j^{(c)}$ is over all sites of the unit cell of the generalized Wigner lattice. Only the factor $|f(k)|^2$ which reflects the dependence of the intensity upon the structure of the generalized Wigner lattice will be discussed here. The $f(k)$ [k given by (17)] have been calculated for the generalized-Wigner-lattice configurations corresponding to a number of different densities ρ using the formula (13). In the absence of any detailed information concerning the V'_{i-j} the ordinary Coulomb form $(R_i - R_j)^{-2}$ has been used for V'_{i-j}.

These calculations showed that most satellites predicted by (17) are of negligible intensity, but a few are relatively strong. For $\rho < \frac{1}{2}$ no strong satellites were found, but for $\rho > \frac{1}{2}$ there were generally one or two strong satellites [the calculation of $f(k)$ is not symmetric against the interchange of electrons and holes]. In Fig. 3 the k corresponding to the strongest satellites have been plotted against ρ (there are matching satellites at $-k$). It will be seen that they form a pattern of straight lines. In general, by far the most intense of the satellites are those on the line ab in Fig. 3; these lie in such a position that the satellite at $b^* - k$ is just at the position usually referred to as $4k_F$. For $\rho \sim 0.8$–0.9, two or three "harmonics" (cd, ef) of this main peak are found (as in Kondo and Yamaji's calculation[8]), and are in some cases almost as intense as the main peak (see Fig. 4). The other most-prominent line is gh, which lies in a position corres-
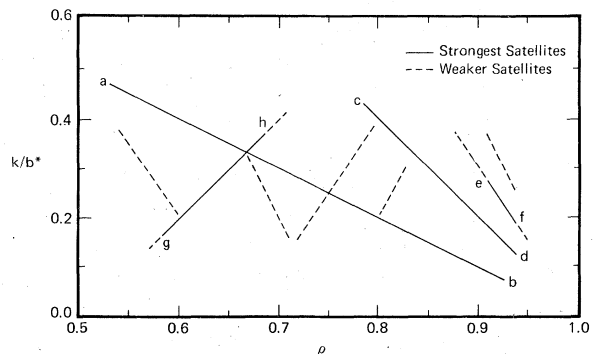

FIG. 3. Positions of strong satellites (displacements k from Bragg spots) due to lattice distortion plotted as a function of ρ.
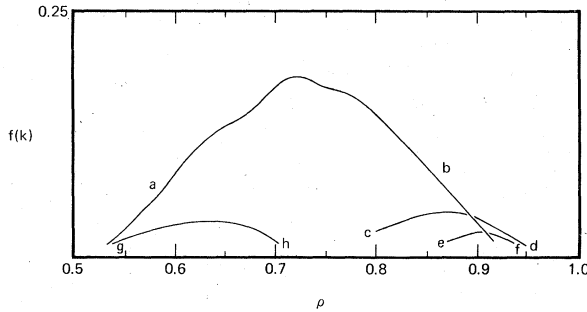
FIG. 4. $f(k)$ (see Sec. V) for strongest satellites as a function of ρ.

ponding to a reflection of the second-harmonic line in $k = \frac{1}{2}b^*$. A number of other, much weaker, lines are also shown in Fig. 3. The intensity of a satellite varies quite strongly with ρ along the lines shown in Fig. 3. In Fig. 4 the intensities $|f(k)|^2$ are plotted as a function of ρ along the principal lines of Fig. 3.

It is not clear how much of the satellite structure discussed above survives when the band motion is taken into account or how much the relative intensities are modified. The ω_k^2 factor in (18) tends to emphasize satellites with small k; on the other hand, as is discussed in Sec. VI, the band motion has exactly the opposite effect of suppressing satellites with small k. Indeed, if the bandwidth is large enough, it may suppress the satellite structure altogether.

VI. BAND-MOTION EFFECTS

The question now arises as to how the preceding results are modified when the band motion is taken into account, i.e., one takes $t \neq 0$ and returns to the study of Hamiltonian (1). Obviously, if t is large enough, the solutions will bear little resemblance to the configurations of Sec. III; however, for a bandwidth $4t \simeq \frac{1}{2}$ eV one may expect, for the reasons explained below, that many of the features of the $t = 0$ limit will be preserved; but even small t can lead to new phenomena not present at $t = 0$.

The first point to note is that if one takes $4t \simeq \frac{1}{2}$ eV, $U - V_1 \simeq 1.5$ eV (from Table I), then there will still be very little double occupancy of sites. For if the band-motion term in (1) causes an electron to hop onto an already occupied site, the interaction energy will be increased by an amount of the order $U - V_1$; since the matrix element for such a hop is t, the probability of a site being doubly occupied is $\sim 2\rho t^2/(U - V_1)^2 \simeq 1\%$ using the above values (the factor 2ρ is a statistical factor). Thus for many (but not all) purposes it would be a good approximation to neglect double occupancy altogether, or, equivalently, take $U = \infty$. This leads

(Sokoloff,[21] Ovchinnikov[7]) to a complete decoupling of the spin and particle motion. The electron spins behave like free spins, giving a Curie-law susceptibility, and the particle motion can be described as that of a gas of spinless fermions with the Hamiltonian

$$H = t \sum_i (c_i^\dagger c_{i+1} + c_{i+1}^\dagger c_i) + \frac{1}{2} \sum_{i \neq j} V_{i-j} n_i n_j , \quad (19)$$

where $n_i = c_i^\dagger c_i$ and $c_i^\dagger, c_i$ are now creation and destruction operators for spinless fermions at site i. Of course such a model provides no information concerning the magnetic behavior of the system; to study this one would have to reintroduce a finite but large U and treat its effects by perturbation theory.

It will be noted that (19) is simply Hamiltonian (5) with a band-motion term introduced, leading to a truly quantum-mechanical problem. In general, one does not know how to determine the spectrum of (19), but there is one rather special case in which considerable progress has been made. This is the case in which $0 = V_2 = V_3 = \cdots$, but V_1 is arbitrary. Then it can be shown (at least in the case of very long chains) that (19) is related to the Ising-Heisenberg problem,[22] i.e., the problem of a chain of $S = \frac{1}{2}$ spins with anisotropic nearest-neighbor coupling, the Hamiltonian being

$$H = \sum_i (S_i^x S_{i+1}^x + S_i^y S_{i+1}^y + \Delta S_i^z S_{i+1}^z) . \quad (20)$$

The relationship is as follows: $\Delta = V_1/2t$, and the states with electron density ρ (electrons/site) correspond to the solutions of (20) with magnetization $M = |\rho - \frac{1}{2}|$ per site. A method of exact solution is known for the problem (20)[23-25] and has been worked out in detail for the cases corresponding to (i) $\Delta = 1$, ρ arbitrary[26]; (ii) $\rho = \frac{1}{2}$, Δ arbitrary,[24,27] and could, in principle, be extended to arbitrary ρ and Δ.

Particularly interesting is the case $\rho = \frac{1}{2}$; in this case it is found that when $\Delta > 1$ there is an energy gap between the ground state and the first excited states,[24,27] implying that the Hamiltonian (19) has an insulator-conductor (Mott) transition at $\Delta = 1$.[7] Thus one may reasonably take $\Delta = 1$, i.e., $V_1 = 2t$ as measuring the point which divides the strong and weak interaction regimes for Hamiltonian (19). Actually, since one had to make the assumption $0 = V_2 = V_3 = \cdots$ to obtain the equivalence with (20), in making such a comparison it would be more correct to replace V_1 by some sort of renormalized value $\hat{V}_1$; $V_1 \rightarrow \hat{V}_1 = V_1 - V_2$ is a reasonable choice. From Table I, column 5, $\hat{V}_1 = 0.5$ eV, giving $\hat{V}_1/2t = 2$ with $4t = 0.5$ eV, so one would be well inside the strong interaction regime with these values.

(a) −X−O−X−O−X−O−X−O−X−

(b) −O−X−O−X−O−X−O−X−O−

(c) −O−X−O−X−X−O−X−O−X−

(d) −O−X−O−X−O−X−X−O−X−

(e) −O−X−O−X−X−X−O−X−O−
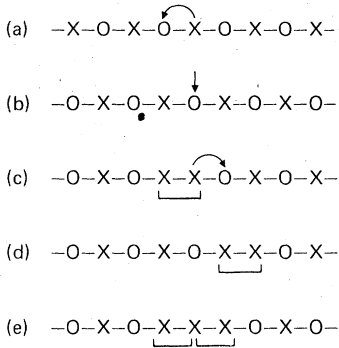
FIG. 5. Band-motion effects (see Sec. VI).

If t is small enough (and the results of the previous paragraph suggest that $4t = 0.5$ eV is small enough), one may think of treating the band-motion term in (19) as a perturbation. If one does this for the case $\rho = \frac{1}{2}$, the leading perturbation would be due to virtual states of the type resulting from the transition indicated in Fig. 5(a). The difference in interaction energy in the ground and virtual state is $D = V_1 - 2V_2 + 2V_3 - \cdots \simeq 0.45$ eV (using Table I, column 5), and the probability of such a transition is $(t/D)^2 \simeq 7\%$. Thus the probability of a "wrong" site being occupied is ~14% (transitions to it could occur from either neighbor).

More interesting is the case in which ρ is a little greater than $\frac{1}{2}$. According to the results of Sec. III, the ground state would then be portions of the $\rho = \frac{1}{2}$ Wigner lattice regularly interrupted by dimer pairs. One may think of the dimer pairs as a kind of domain boundary. For $\rho = \frac{1}{2}$ there is a twofold degeneracy of the ground state corresponding to the two Wigner lattices shown in Figs. 5(a) and 5(b); inspection of Fig. 5(c) shows that the dimer is a domain boundary between these two lattices. Consider now the transition induced by the band term in (19) and indicated in Fig. 5(c); this takes the system to the configuration in Fig. 5(d) which has just the same interaction as in Fig. 5(c) since all that has happened is that the domain boundary has moved two steps. The transition indicated in Fig. 5(c) is thus between two states which are degenerate so far as their interaction energy is concerned. It follows at once that the band term in (19) will cause an isolated dimer to move like a free particle. The dimers will, in fact, have a band structure of the form

$$\epsilon(q) = -2t \cos 2q \; ; \tag{21}$$

$2q$ rather than q occurs because at each transition the dimer hops two lattice spacings.

Thus for densities ρ a little greater than $\frac{1}{2}$ one could think of the system as containing a "dimer gas" with band structure (21). The statistics of

this gas are rather odd, but the principal feature is that one cannot have two dimers in the same place, so they should obey something resembling Fermi statistics. It will be shown below that they behave as though they carried an electric charge equal to $\frac{1}{2}$ the electronic charge, so they can act as current carriers (in fact this mechanism has already been suggested by Lee, Rice, and Klemm[14]).

If one imagines an electron to be injected into the $\rho = \frac{1}{2}$ Wigner lattice at, say, the position indicated in Fig. 5(b), the result will be to create two dimers as shown in Fig. 5(e). Thus each dimer must carry a charge equal to one-half the electronic charge. The cost in interaction energy of adding the extra electron is $E_0 = 2(V_1 + V_3 + \cdots)$. The two dimers may now be expected to move apart by band motion; indeed, one may view the whole process as the addition of two particles to the dimer gas. If the electron is injected with momentum q and the two dimers created have momenta q_1 and q_2, then $q = q_1 + q_2$ and the electron will go in with energy

$$E_0 - 2t(\cos 2q_1 + \cos 2q_2), \quad q_1 + q_2 = q \; , \tag{22}$$

according to (21). Thus there is a two-parameter spectrum for the injection of electrons at $\rho = \frac{1}{2}$.

The equivalent result for the spin problem (20) is already known; in fact, in this case it can be shown[27] that when $\Delta > 1$ the lowest-energy excitations out of the $\rho = \frac{1}{2}$ $(M = 0)$ ground state have a two-parameter spectrum of the form

$$\epsilon_0[(1 - k^2 \cos^2 q_1)^{1/2} + (1 - k^2 \cos^2 q_2)^{1/2}] \; ,$$
$$q_1 + q_2 = q \; , \tag{23}$$

where ϵ_0, k are certain parameters; in the limit $t \to 0$, i.e., $\Delta \to \infty$, (23) passes over into (22).

If one now considers larger ρ, it is more difficult to picture the effects of the band motion. As an example, consider the $\rho = 0.6$ configuration of Fig. 1(a). Since the charge-transfer transition F has so low an energy, it is clear that the dimers will tend to spread out about their positions in the configuration in Fig. 1(a). What is not clear is whether at a bandwidth $4t = 0.5$ eV the dimers will be completely delocalized or whether they will merely oscillate about their positions in Fig. 1(a). If they delocalize and obey something like Fermi statistics, the question arises as to whether a "dimer Kohn anomaly" might arise. These questions can only be answered by a more precise solution for Hamiltonian (19).

Finally, a comment is in order on the way in which the results of Secs. IV and V may be modified by the band motion. As regards the optics, it may first be noted that the band motion of the

dimers has no effect on the relative proportions of neutrals, monomers and dimers upon which the interpretation of the TTF-TCNQ spectrum was based, so this much still stands. Nevertheless, the following question arises: Can one still sensibly identify sites as neutral, monomer, etc.? This is a question of time scales; if one thinks of the band-motion term as a perturbation, then one could picture the system switching between configurations on some time scale determined by the band motion; for example, a site which is a monomer at some instant may as a result of these changes find itself part of a dimer at some later time. If the site switches too quickly between monomer and dimer contexts, a line narrowing phenomenon will occur, which may, for example, collapse the two peaks X, Y [Figs. 2(a) and 2(b)] into a single peak, reflecting the fact that the band motion has destroyed the monomer-dimer distinction. If the band motion is stronger still, the interpretation in terms of intramolecular transitions collapses altogether and must be replaced by a theory of interband transitions. Thus the recognition in the optical spectrum of line structures closely resembling those of the solution spectra suggests that band motion effects are not competing very strongly with the interactions.

As regards the lattice distortions of Sec. V, one may think of the situation as follows. As the band motion causes the system to switch from one configuration to another, the force F_i at a site will fluctuate (with average zero). Whether these forces produce perceptible distortion then depends upon the rate of their fluctuation relative to the lattice relaxation time (approximately a phonon period). If the fluctuations are fast, the lattice cannot follow them and little distortion will occur. This effect tends to suppress distortions with small k (in the notation of Sec. V) most strongly because they have small ω_k. The appearance of the satellite structure discussed in Sec. V thus depends upon the balance between this effect and the ω_k^2 factor appearing in the denominator of (18), the discussion of which really requires a more accurate solution of (19). One may expect, in any case, that the electric field fluctuation will convert the elastic scattering effects of Sec. V into quasielastic scattering.

VII. CONCLUSIONS

It has been concluded on the basis of rather rough estimates of the screening effects (Table I) that in TCNQ charge-transfer salts not only the on-site interactions, but also the interactions between electrons at near-neighbor sites may be of importance in determining the electronic structure.

In the limit in which these interactions are of dominant importance, it has been shown that the lowest energy states at a given charge transfer ρ will be periodic arrangements of the electrons on the chain, the period and detailed arrangement depending upon ρ; these configurations may be regarded as generalizations of the classical Wigner lattice.

It has proved possible, going no farther than this rather idealized model, to give an interpretation of the optical spectra of many TCNQ salts. It has further been shown that such generalized-Wigner-lattice configurations might lead to lattice distortions which would manifest themselves through the appearance of (quasielastic) satellite spots in the x-ray diffraction pattern. In particular, for $\rho > \frac{1}{2}$, a strong satellite may be found in the $4k_F$ position, and in some cases harmonics of this satellite.

Finally, some indication of the way in which these results might be modified by a relatively weak band motion has been given, but it has been concluded that a more-precise treatment of Hamiltonian (19) is called for in this connection.

APPENDIX

Here an outline of the proofs of the statements of Sec. III is given. Suppose one has a chain of N sites and m electrons, so $\rho = m/N$. One wishes to show that the configurations determined by the algorithm of Sec. III minimize the interaction energy (5) subject to (6) when the V_n satisfy (7) and (8). Imagine the chain deformed into a loop, which obviously does not modify the solution in the limit $N \to \infty$. The energy of a configuration is unchanged if one merely rotates it around the loop. One may specify the configuration on the loop (up to an arbitrary rotation) in the following way: number the electrons in order round the loop $1, 2, \ldots, m$ and denote the interval between electrons 1 and 2 by n_1, between electrons 2 and 3 by n_2, etc.; then the set of numbers $\{n_i\} = \{n_1, n_2, \ldots, n_m\}$ specifies the configuration and satisfies the condition $\sum_i n_i = N$. Since the interaction energy is independent of rotations, it must be expressible in terms of the $\{n_i\}$; in fact, one easily finds from (5) that

$$E = \sum_i V(n_i) + \sum_i V(n_i + n_{i+1})$$
$$+ \sum_i V(n_i + n_{i+1} + n_{i+2}) + \cdots , \qquad (A1)$$

where for notational convenience $V(n)$ is now written for V_n, and where, when necessary, one must interpret n_{N+1} as n_1, n_{N+2} as n_2, etc.

One may now associate with any set $\{n_i\}$ specifying a configuration the auxiliary sets of numbers $\{p_i\}$, $\{q_i\}$, ... defined by $p_i = n_i + n_{i+1}$, $q_i = n_i + n_{i+1} + n_{i+2}$, etc. Then (A1) may be written

$$E = U\{n_i\} + U\{p_i\} + U\{q_i\} + \cdots , \qquad \text{(A2)}$$

where

$$U\{x_i\} = \sum_i V(x_i) \qquad \text{(A3)}$$

and the $\{n_i\}$, $\{p_i\}$, $\{q_i\}$, ... satisfy the conditions

$$\sum_i n_i = N, \quad \sum_i p_i = 2N, \quad \sum_i q_i = 3N \cdots . \qquad \text{(A4)}$$

The following lemma is needed: If $\{x_i\}$ $= x_1, x_2, \ldots, x_m$ is a set of integers satisfying

$$\sum_i x_i = X , \qquad \text{(A5)}$$

and $X = mx + a$, where $0 \le a < m$, and the $V(n)$ satisfy (8), then

$$U\{x_i\} \ge (m - a)V(x) + aV(x + 1) . \qquad \text{(A6)}$$

To prove this one needs a result easily deducible from (8), namely,

$$\text{if } s < t, \quad \text{then } V_{s+1} + V_{t-1} \le V_s + V_t . \qquad \text{(A7)}$$

To demonstrate (A6), first suppose that $\{x_i\}$ is a set such that $|x_i - x_j| \le 1$ for all pairs i, j; such a set will be called minimal. For minimal sets, the condition (A5) requires that $m - a$ of the x_i take the

value x and the remaining a the value $x + 1$, so it follows at once for minimal sets from (A3) that the equality in (A6) is satisfied. Now let C be a nonminimal set $\{x_i\}$, so for some s, t one has $x_s > x_t + 1$. Construct the set C' which has all x_i the same as in C except that x_s, x_t are replaced by $x_s - 1$ and $x_t + 1$, respectively. C' still satisfies condition (A5); further, using (A7) one finds $U\{C'\} \le U\{C\}$. If C' is nonminimal, repeat the procedure to obtain a C'' with $U\{C''\} \le U\{C'\}$, and so on until one arrives at a minimal set C_0. Then using the inequalities on U one has $U\{C\} \ge U\{C_0\}$; but since C_0 is minimal, $U\{C_0\}$ is just given by the right-hand side of (A6), and (A6) is demonstrated for arbitrary sets $\{x_i\}$.

One now need only remark that the algorithm of Sec. III is, in fact, nothing more than a construction of a set $\{n_i\}$ such that all the sets $\{n_i\}$, $\{p_i\}$, $\{q_i\}$, ... are minimal subject to conditions (A4). For example, all generalized-Wigner-lattice configurations involve only the intervals n and either $n + 1$ or $n - 1$, so $\{n_i\}$ is minimal; they are all made up of sequences of the form $n^s(n \pm 1)$ and $n^t(n \pm 1)$, where either $t = s + 1$ or $t = s - 1$, so the $\{p_i\}$ can take only the values $2n$ or $2n \pm 1$, and $\{p_i\}$ is minimal, and so on. It follows at once from the lemma that the $U\{n_i\}, U\{p_i\}, \ldots$ for a generalized-Wigner-lattice configuration are less than the $U\{n_i\}, U\{p_i\}, \ldots$, respectively, for any other configuration satisfying (A4). Further, the algorithm of Sec. III automatically constructs a configuration corresponding to the density ρ, so it is confirmed that the generalized Wigner lattice defined by the algorithm of Sec. III is the lowest energy state with that density.

[1]A. J. Berlinsky and J. F. Carolan, Solid State Commun. 15, 795 (1975).

[2]F. Herman, Bull. Am. Phys. Soc. 22, 288 (1977).

[3]J. B. Torrance, B. A. Scott, and F. B. Kaufman, Solid State Commun. 17, 1369 (1975).

[4]J. B. Torrance, in Chemistry and Physics of One-Dimensional Metals, NATO Advanced Study Institute Series (Physics), Vol. 25, edited by H. J. Keller (Plenum, New York, 1977), p. 137.

[5]Z. G. Soos, Ann. Rev. Phys. Chem. 25, 121 (1974).

[6]J. Hubbard, Proc. R. Soc. Lond. A 276, 238 (1963).

[7]A. A. Ovchinnikov, Sov. Phys.-JETP 37, 176 (1973).

[8]J. Kondo and K. Yamaji (unpublished).

[9]E. P. Wigner, Trans. Farad. Soc. Lond. 34, 678 (1938).

[10]J. Tanaka, M. Tanaka, T. Kawai, T. Takabe, and O. Maki, Bull. Chem. Soc. Jpn. 49, 2358 (1976).

[11]H. Johansen, Int. J. Quantum Chem. 9, 459 (1975).

[12]C. K. Ingold, Structure and Mechanism in Organic Chemistry (Bell, London, 1953), Chap. 10.

[13]W. L. McMillan, Phys. Rev. B 14, 1496 (1976).

[14]P. A. Lee, T. M. Rice, and R. A. Klemm, Phys. Rev. B 15, 2984 (1977).

[15]J. B. Torrance and B. D. Silverman, Phys. Rev. B 15, 788 (1977).

[16]C. J. Eckhardt and R. R. Pennelly, Chem. Phys. Lett. 9, 572 (1971).

[17]R.H. Boyd and W. D. Phillips, J. Chem. Phys. 43, 2927 (1965).

[18]P. M. Grant, R. L. Greene, and G. Castro, Bull. Am. Phys. Soc. 20, 496 (1975).

[19]J. B. Torrance, B. A. Scott, B. Welber, and F. B. Kaufman (unpublished).

[20]C. S. Jacobsen, K. Bechgaard, and J. R. Andersen, in The Proceedings of the Conference on Organic Conductors and Semiconductors, Siofok, Hungary, 1976 (unpublished).

[21]J. B. Sokoloff, Phys. Rev. B 2, 779 (1970).

[22]E. Lieb, T. Schultz, and D. Mattis, Ann. Phys. (N.Y.) 16, 407 (1961).

[23]H. Bethe, Z. Phys. 71, 205 (1931).

[24]J. des Cloizeaux and M. Gaudin, J. Math. Phys. 7, 1384 (1966).

[25]M. Gaudin, Phys. Rev. Lett. 26, 1303 (1971).

[26]R. B. Griffiths, Phys. Rev. 133, A768 (1964).

[27]J. D. Johnson and B. M. McCoy, Phys. Rev. A 4, 1613 (1972).

[28]J. P. Pouget, S. K. Khanna, F. Denoyer and R. Comès, Phys. Rev. Lett. 37, 437 (1976).

[29]S. Kagoshima, T. Ishiguro, and H. J. Anzai, J. Phys. Soc. Jpn. 41, 2061 (1976).

[30]K. Ukei and I. Shirotani, Communications on Physics 2, 159 (1977).